BRAIN REPORT

Mechanisms of imbalanced frontostriatal functional connectivity in obsessive-compulsive disorder

Sebastien Naze,[1] Luke J. Hearne,[1] James A. Roberts,[1] Paula Sanz-Leon,[1] Bjorn Burgher,[1] Caitlin Hall,[1] Saurabh Sonkusare,[1] Zoie Nott,[1] Leo Marcus,[1] Emma Savage,[1] Conor Robinson,[1] Ye Ella Tian,[2] Andrew Zalesky,[2] Michael Breakspear[3] and Luca Cocchi[1]

The diagnosis of obsessive-compulsive disorder (OCD) has been linked with changes in frontostriatal resting-state connectivity. However, replication of prior findings is lacking, and the mechanistic understanding of these effects is incomplete. To confirm and advance knowledge on changes in frontostriatal functional connectivity in OCD, participants with OCD and matched healthy controls underwent resting-state functional, structural and diffusion neuroimaging.

Functional connectivity changes in frontostriatal systems were here replicated in individuals with OCD ($n = 52$) compared with controls ($n = 45$). OCD participants showed greater functional connectivity ($t = 4.3$, $P_{FWE} = 0.01$) between the nucleus accumbens (NAcc) and the orbitofrontal cortex (OFC) but lower functional connectivity between the dorsal putamen and lateral prefrontal cortex ($t = 3.8$, $P_{FWE} = 0.04$) relative to controls. Computational modelling suggests that NAcc-OFC connectivity changes reflect an increased influence of NAcc over OFC activity and reduced OFC influence over NAcc activity (posterior probability, $Pp > 0.66$). Conversely, dorsal putamen showed reduced modulation over lateral prefrontal cortex activity ($Pp > 0.90$). These functional deregulations emerged on top of a generally intact anatomical substrate.

We provide out-of-sample replication of opposite changes in ventro-anterior and dorso-posterior frontostriatal connectivity in OCD and advance the understanding of the neural underpinnings of these functional perturbations. These findings inform the development of targeted therapies normalizing frontostriatal dynamics in OCD.

1 Department of Mental Health and Neuroscience, QIMR Berghofer Medical Research Institute, Brisbane 4006, Australia
2 Melbourne Neuropsychiatry Centre, Department of Psychiatry, The University of Melbourne and Melbourne Health, Melbourne 3053, Australia
3 College of Engineering Science and Environment, College of Health and Medicine, University of Newcastle, Callaghan 2308, Australia

Correspondence to: Sebastien Naze
QIMR Berghofer
300 Herston Road, Brisbane, QLD 4006, Australia
E-mail: sebastien.naze@qimrberghofer.edu.au

Correspondence may also be addressed to: Luca Cocchi
E-mail: luca.cocchi@qimrberghofer.edu.au

Keywords: cortico-striatal; DCM; nucleus accumbens; OCD; connectivity

Received August 11, 2022. Revised October 13, 2022. Accepted October 30, 2022. Advance access publication November 16, 2022

Introduction

Evidence from preclinical[1,2] and clinical[3–5] studies highlight changes in frontostriatal circuits in obsessive-compulsive disorder (OCD). In a seminal paper, Harrison *et al.*[4] reported distinct patterns of fronto-striatal resting-state connectivity along the ventro-dorsal axis in OCD. Importantly, their results suggested a linear association between symptom severity and resting-state functional connectivity between the nucleus accumbens (NAcc) and the orbitofrontal cortex (OFC). These findings are consistent with data from invasive studies in humans[6,7] and animal models,[2] suggesting a causal effect of altered frontostriatal functional connectivity on OCD pathology. Accordingly, subcortical deep brain stimulation targeting cortico-striato-thalamic systems has been shown to alleviate OCD symptoms[8] and deficits in mood and cognition.[9] However, the results from Harrison and colleagues[4] lack independent validation. Moreover, whether changes in resting-state functional connectivity emerge from an altered influence of striatal activity over the frontal cortex, or modified frontal cortex influence over striatal activity, remains to be elucidated.[10] Finally, it remains unclear whether OCD is associated with anatomical abnormalities supporting these dysfunctional frontostriatal systems.

We combined neuroimaging and computational modelling to replicate and extend knowledge of OCD frontostriatal systems. Neuroimaging and phenotypic data were acquired from an original sample of individuals with OCD and matched healthy controls (Table 1). We sought to: (i) replicate the changes in frontostriatal functional connectivity described by Harrison *et al.*[4]; (ii) infer the neural interactions causing these pathological patterns of functional connectivity; (iii) assess possible alterations in their anatomical underpinnings; and (iv) test for associations between neuroimaging features and OCD symptom severity.

Materials and methods

Participants

Participants with a clinical diagnosis of OCD for at least 12 months were recruited across Australia as part of a clinical trial (ACTRN12616001687482). The diagnosis of OCD was independently confirmed by a board-certified psychiatrist (M.B. or B.B.). Neurocognitive assessments (Table 1) were performed by trained provisional psychologists. The OCD cohort was compared to age-, gender- and handedness-matched controls (Table 1). Forty-three OCD participants were prescribed with stable psychoactive medication for at least 1 month before testing, while nine were free from psychoactive medication. All participants were between 18 and 50 years old. Exclusion criteria were a history of psychotic disorders, suicide attempts, manic episodes, seizures, neurological disorders, traumatic head injuries, substance abuse disorders and contraindications to MRI.

The study was approved by the Human Research Ethics Committee of QIMR Berghofer (P2253). Written informed consent was obtained from all participants.

Neuroimaging data acquisition

Brain imaging data were acquired on a 3 T Siemens Prisma MR scanner equipped with a 64-channel head coil located at the Herston Imaging Research Facility, Brisbane, Australia (details in the Supplementary material).

Neuroimaging data preprocessing and analysis

Functional MRI

The functional brain images were pre-processed using a combination of fMRIprep (version 20.2.1)[12] and FMRIB's ICA-based X-noiseifier (ICA-FIX)[13] (Supplementary material). Statistical testing was constrained to the four cortico-striatal systems affected by OCD described in Shephard *et al.*[1] Frontal masks for each cortico-striatal system were generated by matching frontal regions' names described in Shephard *et al.*[1] to the cortical parcels defined by Schaefer *et al.*[14] using the parcel names provided in the 400 regions' atlas (Supplementary Table 1 and Supplementary Fig. 1). Functional connectivity was computed between the average functional MRI (fMRI) signal within a striatal seed and comprising its corresponding frontal mask using Pearson's correlation. Striatal seeds were defined as per Harrison *et al.*[4] and Di Martino *et al.*[15]: spheres of 3.5 mm radius centred on Montreal Neurological Institute (MNI) coordinates corresponding to the nucleus accumbens (NAcc: $x = \pm 9$, $y = 9$, $z = -8$), the dorsal caudate (dCaud: $x = \pm 13$, $y = 15$, $z = 9$), the dorsal putamen (dPut: $x = \pm 28$, $y = 1$, $z = 3$) and the ventral putamen (vPut: $x = \pm 20$, $y = 12$, $z = -3$). Group differences in functional connectivity were tested independently for each of the four pairs of striato-cortical regions using FSL randomise[16] (5000 permutations). Significant clusters were identified using the threshold-free cluster enhancement method (TFCE) and corrected for multiple comparisons using a family-wise error rate of maximum 5% ($P_{FWE} < 0.05$).

A confirmatory analysis was performed using whole-brain cortical masks computed using data from the Human Connectome Project (HCP)[17] (Supplementary material).

Dynamic causal modelling and parametric empirical Bayes

We used dynamic causal modelling (DCM) to model neural dynamics in each group. DCM uses variational Bayes to fit a biophysical model of neural dynamics and associated blood oxygen level-dependent (BOLD) responses to the fMRI timeseries.[18] DCM models interaction within and between the underlying neural populations using dynamic state equations. The units of coupling are rate constants measured in hertz for recurrent connections and log-scaled arbitrary units for between-region interactions. Cross-spectral density features were used to invert the model as this approach has proven its validity for the efficient estimation of resting-state connectivity.[19] Individual time series were extracted from the three striatal seeds and their corresponding three statistically significant frontal clusters of interest (Fig. 1 and Supplementary Fig. 2), resulting in a total of six volumes of interest (VOIs). Specifically, the frontal VOIs were created from the intersection of a cluster derived from the group level analysis and a 3.5 mm sphere centred at the individual's peak functional connectivity within the cluster. This ensured that VOIs were of similar sizes across the six regions (20 voxels, or 180 mm^3) while also maximizing signal-to-noise ratio at subject level.

Effective connectivity weights were estimated between a single striatal seed and its corresponding cortical cluster (Fig. 1A and Supplementary Fig. 2). Group differences were tested within each frontostriatal system using recurrent (self), feedforward (striatum to frontal cortex) and feedback (frontal cortex to striatum) connections (Fig. 1C). As a complementary analysis, fully connected DCMs, modelling effective connectivity between all striatal and frontal VOIs, were also estimated (Supplementary Fig. 3A). To test for between-group effects in neural couplings, we used parametric

Table 1 Socio-demographic and clinical characteristics of the sample

	Controls ($n = 45$)	OCD ($n = 52$)	P-value
Age, years	32.5 (8.7)	30.2 (7.9)	0.18
Gender, % female	40	44	0.68
Handedness, % right	96	85	0.08
IQ-Full scale[a]	112.7 (11.3)	106.0 (12.5)	0.007
OBQ	116.5 (47.1)	196.8 (51.2)	<0.001
OCI-R	5.5 (7.1)	33.2 (14.6)	<0.001
HAM-A	2.9 (3.1)	19.5 (8.6)	<0.001
HADS Anxiety; Depression	4.8 (3.7); 2.2 (2.3)	13.3 (4.7); 8.2 (4.8)	<0.001
MADRS	2.9 (3.5)	19.5 (10.4)	<0.001
Y-BOCS Total	1.8 (3.0)	25.3 (5.2)	<0.001
Symptoms dimensions	Absent–Mild–Severe		
Sexual/Religious	100–0–0%	31–39–30%	<0.00001
Symmetry/Ordering	100–0–0%	51–39–10%	<0.00001
Hoarding	100–0–0%	61–31–8%	<0.00001
Contamination/Cleaning	98–2–0%	12–16–72%	<0.00001
Aggressive/Checking	89–9–2%	6–8–86%	<0.00001

Values are presented as mean (standard deviation) unless otherwise stated. *P*-values relate to Student's *t*-test for continuous data and χ^2 test for categorical data. Y-BOCS symptoms dimensions computed as in previously reported.[4,11] HADS = Hospital Anxiety and Depression scale; HAM-A = Hamilton Anxiety Rating Scale; MADRS = Montgomery-Asberg Depression rating scale; OBS = Obsessional Beliefs Questionnaire; OCI-R = Obsessive Compulsive Inventory-Revised; Y-BOCS = Yale-Brown Obsessive Compulsive Scale.
[a]Wechsler Adult Intelligence Scale (WAIS-IV).

empirical Bayes (PEB).[20] The PEB scheme starts by estimating the parameters of interest from all subjects. Bayesian model comparison is subsequently performed using subject-specific model parameters (first level) to infer group effects, with the sample mean and group-specific deviations from this mean included as regressors. Next, Bayesian model reduction is performed over the group-specific parameters (second level). This approach prunes parameters that do not contribute to the model evidence via a greedy search.[21] Given the Bayesian framework of PEB, differences in effective connectivity between the groups are reported as posterior probabilities (Pp).

Diffusion MRI

Diffusion images were corrected for B0 field inhomogeneities, eddy current and inter-volume motion using top-up and eddy tools from FSL 6.0. Individual images were visually checked, and four participants (one control and three OCD) were discarded due to poor data quality. Fibre orientations densities (FODs) were estimated using constrained spherical deconvolution (CSD) provided by MRtrix3[22] and implemented in QSIPrep (v.0.13.0) with default parameters.[23] One hundred million streamlines were reconstructed for each subject using probabilistic tractography (iFod2 algorithm), seeded from the grey-white matter boundary with minimum and maximum lengths of 3 and 25 cm, respectively, and a maximum angle of 30° between consecutive points. Track density (TD) maps[24] were computed using VOIs centred on the functional seeds (MNI coordinates for right NAcc: x = 9, y = 9, z = −8; right dPut: x = 28, y = 1, z = 3; left vPut: x = −20, y = 12, z = −3) and the peak of their associated cortical clusters of interest [right OFC: x = 23, y = 57, z = −6; right lateral prefrontal cortex (lPFC): x = 53, y = 13, z = 19; left dorsal prefrontal cortex (dPFC): x = −24, y = 55, z = 35] (Fig. 1 and Supplementary Fig. 2). To ensure that the frontal VOIs located in grey matter overlap with tracks terminating at the grey-matter–white-matter boundary, we used a sphere of 6 mm radius all VOIs. The left dPFC cluster being located on the pial surface, for this volume we used a 12 mm sphere radius to ensure that the VOI did encompass areas of the grey-matter–white-matter boundary where tracks terminate. Subject and pathway-specific masks were created from these TD maps using a variable threshold spanning from the 30th to the 90th percentile of TD distribution. The average generalized fractional anisotropy (GFA) over these masks were compared across groups. A systematic analysis was performed independently for each TD threshold value without showing significant difference. In individuals without tracks within a pathway, the group average mask on this pathway was used instead.

Data and code availability

Raw data were generated at QIMR Berghofer. Derived data supporting the findings of this study are available from the corresponding author on request. The code of the analysis is publicly available on the group Github repository at https://github.com/clinical-brain-networks/OCD_Naze_et_al_2022_Brain.

Results

Replication of resting state functional connectivity changes in frontostriatal systems in OCD

We computed resting state functional connectivity between four striatal seeds and their associated four frontal grey matter regions corresponding to the functionally relevant cortico-striatal systems described as being implicated in OCD[1] (Supplementary Fig. 1A and B). Group-comparisons were computed within these masks using non-parametric inference (see 'Materials and methods' section).

The ensuing results replicated the 'greater' functional connectivity between the right NAcc and the right OFC in OCD compared with healthy controls ($t = 4.3$, $P_{FWE} = 0.01$, Cohen's $d = 0.84$; Fig. 1A and B). These analyses also replicated a 'decrease' in functional connectivity between the dPut and the lPFC ($t = 3.8$, $P_{FWE} = 0.04$, $d = 0.64$) in OCD. A complementary analysis, performed using whole-brain grey matter cortical masks derived from 1080 healthy young adults, confirmed those results (Supplementary Figs 1C and 4). Moreover, an additional analysis suggests that our results are unlikely to be related to medication status (Supplementary Fig. 5).

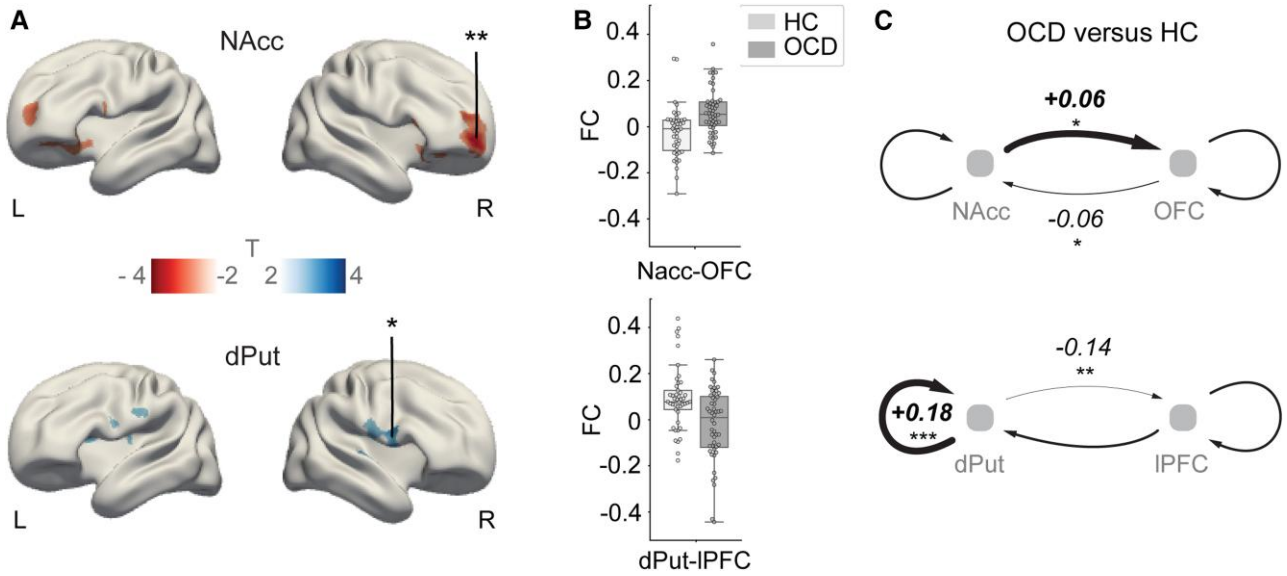

Figure 1 Functional and effective connectivity differences in OCD versus healthy controls. (**A**) Main effect of group: increased (T < 0) and decreased (T > 0) functional connectivity in OCD (|t| > 2.5). *$P_{FWE} = 0.04$, **$P_{FWE} = 0.01$). MNI coordinates for NAcc seed: x = ±9, y = 9, z = −8; dPut seed: x = ±28, y = 1, z = 3. R = right hemisphere; L = left hemisphere. (**B**) Pearson correlation values (functional connectivity, FC) between fMRI signals in the seed regions and the highlighted clusters denoted by asterisks in **A**. Boxes extend from first to third quartile, whiskers span 1.5 of the interquartile range and individuals' FC values are marked by small circles. (**C**) Group differences in 'effective' connectivity between seed regions and cortical clusters depicted by asterisks in **A**. Plus symbols and thick lines, and minus sign symbols and thin lines indicate deviations relative to the mean across groups inferred through DCM. *Pp > 0.66 (moderate); **Pp > 0.9 (strong); ***Pp > 0.95 (very strong). OFC peak coordinates: x = 23, y = 57, z = −6; lPFC peak coordinates: x = 53, y = 13, z = 19. HC = healthy controls.

Functional connectivity differences in a third pathway comprising the vPut and the dPFC were of medium effect but not statistically significant when correcting for multiple comparisons ($t = 3.5$, $P_{uncorr} < 0.0005$, $P_{FWE} = 0.15$, $d = 0.63$) (Supplementary Fig. 2A and B). While our results indicated a difference in the right hemisphere, no group by hemisphere interaction was detected (as per Harrison *et al.*[4]). Statistical maps of significant clusters reported in Harrison *et al.*[4] are provided in Supplementary Fig. 6.

Changes in neural interactions underlying altered functional connectivity in OCD

We used spectral DCM (see 'Materials and methods' section) to infer changes in the neural interactions between the frontal and striatal brain regions comprising the two systems of interest (Fig. 1A and B). Group differences in recurrent (self), feedforward (striatum to frontal cortex) and feedback (frontal cortex to striatum) effective connectivity were estimated using PEB (see 'Materials and methods' section). These analyses revealed increased feedforward and reduced feedback coupling in OCD compared to controls in the NAcc-OFC system (±0.06 log scaled a.u., Pp > 0.66). Conversely, the dPut-PFC system showed decreased feedforward (−0.14 log scaled a.u., Pp > 0.9) and increased recurrent (dPut: +0.18 Hz, Pp > 0.95) effective connectivity in OCD (Fig. 1C). Exploratory analyses in the vPut-dPFC system showed that changes in effective connectivity mirrored those observed for the dPut-lPFC system (−0.19 log scaled a.u. in feedforward, +0.12 Hz recurrent within dPFC connections, Pp > 0.95) (Supplementary Fig. 2C).

Group-differences in effective connectivity remained consistent when using a fully connected DCM (i.e. whereby connectivity is assessed between all the clusters of interest combined from Fig. 1 and Supplementary Fig. 2). Note that cross-pathways interactions were also modelled (Supplementary Fig. 3). Notably, the increased NAcc coupling to frontal regions in this model extends dorso-laterally (Pp > 0.99), supporting a core role of NAcc functional deregulation in OCD pathology.

Anatomical underpinning of changes in spontaneous frontostriatal connectivity in OCD

We used diffusion MRI-derived tractography to generate within-subject structural connectivity masks comprising the right NAcc-OFC and the right dPut-lPFC pathways (Fig. 2A). Generalized fractional anisotropy was calculated within these masks for each individual to test for anatomical difference between groups (see 'Materials and methods' section). The two groups did not statistically differ in GFA measure for the two pathways (Fig. 2B; Kolmogorov–Smirnov test, $P_{uncorr} > 0.2$, $d = 0.2$). We also investigated possible changes in the anatomical substrate of the left vPut-dPFC system without significant group differences. These results were robust to changes in preprocessing thresholds (see 'Materials and methods' section). Confirmatory analyses adopting alternative measures of structural connectivity likewise did not reveal significant differences (Supplementary Fig. 7).

Association between symptoms and functional connectivity in OCD

There was no significant association between OCD symptoms severity (total Y-BOCS score) and NAcc-OFC functional connectivity in our sample. We hence could not validate the corresponding findings reported in Harrison *et al.*[4] (Fig. 2C). Additional explorative correlations with Obsessive Beliefs Questionnaire, Obsessive-Compulsive Inventory-Revised, Hamilton Anxiety Rating Scale, Montgomery-Asberg Depression Rating Scale and Hospital Anxiety and Depression Scale scores (Table 1) did not reveal any significant brain-behaviour associations.

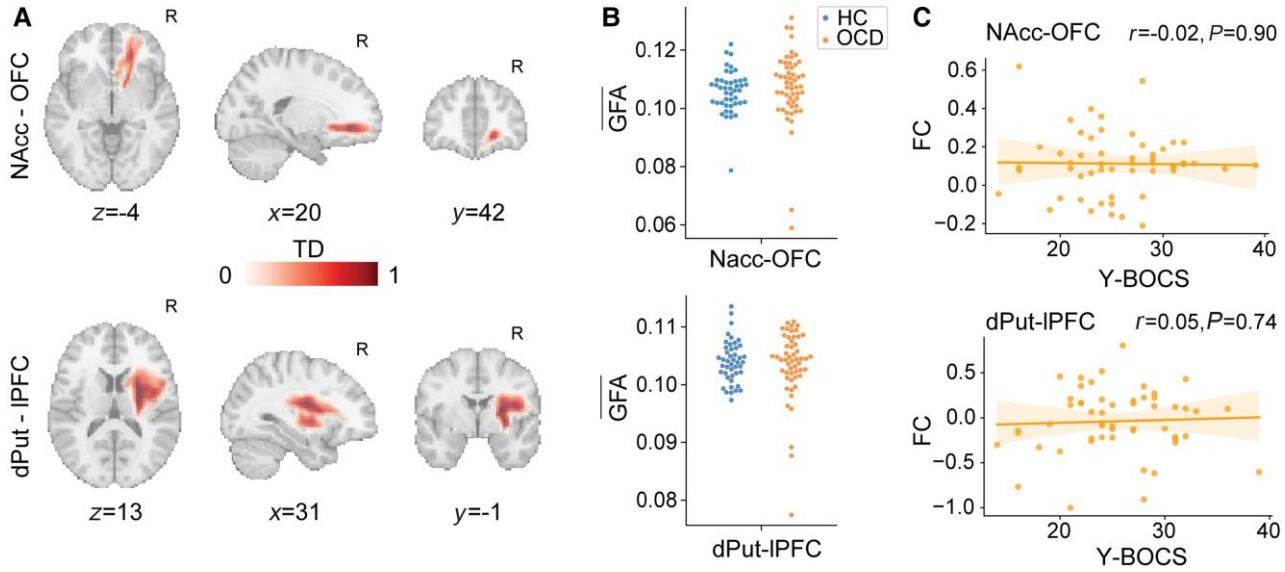

Figure 2 Anatomical differences and brain-symptoms associations in the frontostriatal pathways supporting functional systems affected by OCD. (**A**) Number of tracts in each voxel, computed and normalized for each subject (TD). NAcc-OFC and dPut-lPFC ipsilateral pathways shown. For illustration purposes, the TD maps were averaged across subjects. R = right hemisphere. (**B**) GFA in each frontostriatal pathway of interest, averaged across voxels encompassing the structural connectivity masks (**A**). (**C**) Linear regression between behavioural score (Y-BOCS) and functional connectivity in the two pathways of interest. NAcc (right hemisphere), OFC (right), lPFC (right).

Discussion

Our results provide further evidence of stronger ventro-anterior but weaker dorso-posterior frontostriatal functional connectivity at rest in OCD.[4] We extend this knowledge by showing that functional connectivity changes in the NAcc-OFC system in OCD are associated with greater ventro-striatal influence over orbitofrontal activity and a reduced influence of orbitofrontal activity over the ventral striatum. In contrast, the putamen hypo-modulates two distinct clusters in the posterior dorsolateral frontal cortices. Previous preclinical work suggested that a chronic increase in ventromedial striatal activity leads to pathological activity and plasticity in the frontal cortex, and OCD-like behaviour.[2] Our findings support this hypothesis and extend it by suggesting that OCD likely emerges from a more complex functional imbalance affecting distinct corticostriatal systems.

While our sample size was comparable or larger than previous studies including Harrison *et al.*[4] and Vaghi *et al.*,[9] we did not replicate the positive relationship between symptom severity and NAcc-OFC functional connectivity. Considering the effect of $r = 0.76$ and other measures reported by Harrison *et al.*,[4] our sample size of 52 has a statistical power of over 0.90 to detect this same effect. In contrast, the size of this effect was negligible, suggesting inadequate power was not the cause of our failure to replicate. This result may reflect the different clinical characteristics of the samples. For example, in Harrison *et al.*,[4] a large proportion of individuals had aggressive/checking symptoms, while our sample presented with a higher level of contamination/cleaning symptoms (Table 1). This divergence motivates future studies characterizing the neural substrates underpinning the heterogeneous symptoms comprising the diagnosis of OCD.

Previous studies have suggested that OCD is linked to structural changes in brain regions and connections encompassing the frontostriatal systems.[25,26] Here, we did not observe significant changes in structural connectivity between groups using tractography measures. This does not rule out the presence of abnormal structural connectivity in OCD,[27] but suggests that such changes are unlikely to drive the observed functional deregulations.

The validation of distinct changes in OCD frontostriatal functional connectivity in an independent replication strengthens the targeting of these regions in neuromodulatory therapies. Specifically, our results support deep brain stimulation interventions reducing NAcc modulatory influence on the OFC.[7,8,28] The reported differences in effective connectivity also add mechanistic insights to the altered balance of excitation and inhibition in the associated systems. These findings are important to assist the clinical translation of new non-invasive brain stimulation methods including focused ultrasound stimulations.[29] These emerging techniques may allow the targeted change of distinct striatal outputs via the modulation of excitatory or inhibitory neural populations.[30] Finally, the relative preservation of structural connectivity suggests that OCD is largely related to functional disruptions that are likely remediable by pharmacotherapy and neuromodulation.

Acknowledgements

Data were provided (in part) by the Human Connectome Project, WU-Minn Consortium (Principal Investigators: David Van Essen and Kamil Ugurbil; 1U54MH091657) funded by the 16 NIH Institutes and Centers that support the NIH Blueprint for Neuroscience Research; and by the McDonnell Center for Systems Neuroscience at Washington University.

Funding

This work was supported by the Australian National Health and Medical Research Council (NHMRC GN2001283, L.C. and S.N.) and philantropic donations from the Perrin and Dowling family foundations. M.B. and A.Z. were supported by research fellowships from the NHMRC (APP1136649 and APP1118153, respectively).

Competing interests

L.C., B.B., L.J.H, C.R. and A.Z. are involved in a not-for-profit clinical neuromodulation centre (Qld. Neurostimulation Centre). This centre had no role in the present trial.

Supplementary material

Supplementary material is available at *Brain* online.

References

1. Shephard E, Stern ER, van den Heuvel OA, *et al*. Toward a neurocircuit-based taxonomy to guide treatment of obsessive-compulsive disorder. *Mol Psychiatry*. 2021;26:4583-4604.
2. Ahmari SE, Spellman T, Douglass NL, *et al*. Repeated cortico-striatal stimulation generates persistent OCD-like behavior. *Science*. 2013;340:1234-1239.
3. Dunlop K, Woodside B, Olmsted M, Colton P, Giacobbe P, Downar J. Reductions in cortico-striatal hyperconnectivity accompany successful treatment of obsessive-compulsive disorder with dorsomedial prefrontal rTMS. *Neuropsychopharmacology*. 2016; 41:1395-1403.
4. Harrison BJ, Soriano-Mas C, Pujol J, *et al*. Altered corticostriatal functional connectivity in obsessive-compulsive disorder. *Arch Gen Psychiatry*. 2009;66:1189-1200.
5. van den Heuvel OA, Veltman DJ, Groenewegen HJ, *et al*. Frontal-striatal dysfunction during planning in obsessive-compulsive disorder. *Arch Gen Psychiatry*. 2005;62:301-309.
6. Haber SN, Yendiki A, Jbabdi S. Four deep brain stimulation targets for obsessive-compulsive disorder: Are they different? *Biol Psychiatry*. 2021;90:667-677.
7. Figee M, Luigjes J, Smolders R, *et al*. Deep brain stimulation restores frontostriatal network activity in obsessive-compulsive disorder. *Nat Neurosci*. 2013;16:386-387.
8. Tyagi H, Apergis-Schoute AM, Akram H, *et al*. A randomized trial directly comparing ventral capsule and anteromedial subthalamic nucleus stimulation in obsessive-compulsive disorder: Clinical and imaging evidence for dissociable effects. *Biol Psychiatry*. 2019;85:726-734.
9. Vaghi MM, Vértes PE, Kitzbichler MG, *et al*. Specific frontostriatal circuits for impaired cognitive flexibility and goal-directed planning in obsessive-compulsive disorder: Evidence from resting-state functional connectivity. *Biol Psychiatry*. 2017;81:708-717.
10. Ahmari SE, Rauch SL. The prefrontal cortex and OCD. *Neuropsychopharmacology*. 2022;47:211-224.
11. Mataix-Cols D, Rauch SL, Manzo PA, Jenike MA, Baer L. Use of factor-analyzed symptom dimensions to predict outcome with serotonin reuptake inhibitors and placebo in the treatment of obsessive-compulsive disorder. *Am J Psychiatry*. 1999; 156:1409-1416.
12. Esteban O, Markiewicz CJ, Blair RW, *et al*. fMRIPrep: A robust preprocessing pipeline for functional MRI. *Nat Methods*. 2019;16: 111-116.
13. Griffanti L, Salimi-Khorshidi G, Beckmann CF, *et al*. ICA-based artefact removal and accelerated fMRI acquisition for improved resting state network imaging. *Neuroimage*. 2014;95: 232-247.
14. Schaefer A, Kong R, Gordon EM, *et al*. Local-global parcellation of the human cerebral cortex from intrinsic functional connectivity MRI. *Cereb Cortex*. 2018;28:3095-3114.
15. Di Martino A, Scheres A, Margulies DS, *et al*. Functional connectivity of human striatum: A resting state fMRI study. *Cereb Cortex*. 2008;18:2735-2747.
16. Winkler AM, Ridgway GR, Webster MA, Smith SM, Nichols TE. Permutation inference for the general linear model. *Neuroimage*. 2014;92:381-397.
17. Van Essen DC, Ugurbil K, Auerbach E, *et al*. The human connectome project: A data acquisition perspective. *Neuroimage*. 2012; 62:2222-2231.
18. Friston KJ, Harrison L, Penny W. Dynamic causal modelling. *Neuroimage*. 2003;19:1273-1302.
19. Razi A, Kahan J, Rees G, Friston KJ. Construct validation of a DCM for resting state fMRI. *Neuroimage*. 2015;106:1-14.
20. Friston K, Zeidman P, Litvak V. Empirical Bayes for DCM: A group inversion scheme. *Front Syst Neurosci*. 2015;9:164.
21. Friston KJ, Litvak V, Oswal A, *et al*. Bayesian Model reduction and empirical Bayes for group (DCM) studies. *Neuroimage*. 2016;128: 413-431.
22. Tournier JD, Smith R, Raffelt D, *et al*. MRtrix3: A fast, flexible and open software framework for medical image processing and visualisation. *Neuroimage*. 2019;202:116-137.
23. Cieslak M, Cook PA, He X, *et al*. QSIPrep: An integrative platform for preprocessing and reconstructing diffusion MRI data. *Nat Methods*. 2021;18:775-778.
24. Calamante F, Tournier JD, Jackson GD, Connelly A. Track-density imaging (TDI): Super-resolution white matter imaging using whole-brain track-density mapping. *Neuroimage*. 2010;53:1233-1243.
25. Park H, Kim M, Kwak YB, *et al*. Aberrant cortico-striatal white matter connectivity and associated subregional microstructure of the striatum in obsessive-compulsive disorder. *Mol Psychiatry*. Published online 26 May 2022.
26. Piras F, Piras F, Chiapponi C, Girardi P, Caltagirone C, Spalletta G. Widespread structural brain changes in OCD: A systematic review of voxel-based morphometry studies. *Cortex*. 2015;62: 89-108.
27. Maziero MP, Seitz-Holland J, Cho KIK, *et al*. Cellular and extracellular white matter abnormalities in obsessive-compulsive disorder: A diffusion magnetic resonance imaging study. *Biol Psychiatry Cogn Neurosci Neuroimaging*. 2021;6:983-991.
28. Li N, Baldermann JC, Kibleur A, *et al*. A unified connectomic target for deep brain stimulation in obsessive-compulsive disorder. *Nat Commun*. 2020;11:3364.
29. Folloni D. Ultrasound neuromodulation of the deep brain. *Science*. 2022;377:589.
30. Yu K, Niu X, Krook-Magnuson E, He B. Intrinsic functional neuron-type selectivity of transcranial focused ultrasound neuromodulation. *Nat Commun*. 2021;12:2519.